MECHTA
International Journal Of Mechanical Engineering Technologies & Applications
V05 N.1
ISSN 2722-3213 articles 7, pp. 63 – 72, 2024

OPTIMIZATION OF SHELL AND TUBE HEAT EXCHANGER DESIGN WITH INCLINED BAFFLES

Aulia Rahman [1)] ✉ , Winarto [1)], Eko Siswanto [1)]

[1)] **Mechanical Engineering Department**
Brawijaya University
MT. Haryono, 167
Malang, Jawa-Timur, INDONESIA
aulia.rahman1403@yahoo.ac.id.

Abstract

Shell and tube heat exchanger (STHeX) design development continues to be carried out to increase the effectiveness of a system. One way is to investigate the optimal baffle design. The new structure of STHeX with Inclined-Segmental Baffles is further investigated. The experiment was carried out using the numerical method Computing Fluid Dynamics (CFD) software with three-dimensional modeling. The results show that the heat change coefficient value is lower than conventional STHeX, However, the pressure drop value is reduced quite significantly. Therefore, it is necessary to know the overall heat transfer coefficient value per pressure loss (U/ΔP). Hence, we get U/ΔP values of 0.9 and 0.68 for STHeX with Inclined-Segmental Baffle and conventional STHeX, respectively. Thus, there is a significant increase ranging from 37-34%. It is concluded that STHeX with Inclined-Segmental baffles increases the U/ΔP value significantly compared to conventional STHeX.

Keywords: *Heat Exchanger, CFD, Numerical Simulation, Optimization.*

1. INTRODUCTION

A heat exchanger is a device to utilize the temperature difference between two or more fluids to transfer heat energy between the two fluids [1]. In industry there is use of heat exchange equipment starting from the oil and gas industry, refrigeration, air conditioning, petrochemicals, power plants, medicine industry, metallurgy, aerospace and many others [2]. There are many types of heat exchangers, one of the most common is the Shell and Tube Heat Exchanger (STHeX). Simplicity of design, ease of fabrication and ease of maintenance are the main reasons why STHeX is widely chosen, however there are still many shortcomings of conventional STHeX with a single baffle, namely high pressure drop, dead zones and high vibration [3]–[6]. With these various disadvantages, many researchers have carried out developments on the shell side, one of which is by varying the baffle design [7] [8].

With the development of numerical computing, researchers can easily see phenomena that occur in fluid flow [9]. As done by Gu, Luo, et al [10] conducted numerical method research regarding baffle variations called trapeziodal-like tilted baffles. It was found that this variation resulted in a significant increase in the heat transfer coefficient compared to the others. Several years later Gu, Chen, et al [3] conducted research by looking at the dead zones on several types of baffles. Research with variations in baffle configuration was carried out by Wen et al [11] to see heat transfer on STHeX using the Computational Fluid Dynamic (CFD) numerical method. Then it was discovered that there was an increase in heat transfer without a significant increase in pressure drop. Other geometry optimizations were also examined on STHeX by changing the baffle configuration and modifying the tube installed

Corresponding Author:
✉ **Aulia Rahman**
aulia.rahman1403@yahoo.ac.id
Received on: 2024-01-04
Revised on: 2024-01-15
Accepted on: 2024-01-22

DOI: 10.21776/MECHTA.2024.005.01.7

on STHeX. It was found that the heat transfer and heat transfer coefficient increased with the modifications made [12].

After being developed by many parties, the author is interested in continuing the research carried out by testing the torsional flow type of STHeX by varying the baffle. STHeX testing was carried out using CFD simulation. With the aim of obtaining an optimal design in terms of total heat coefficient and pressure drop.

2. MATERIALS AND METHODS

The simulation was carried out by looking at the relationship between the fluid flow side of the shell and the pressure drop and heat gain coefficient. The software used to carry out the simulation is ANSYS Workbench. Cold fluid flows into the shell side and hot fluid flows into the tube side. The fluid used in this research is water on both the shell and tube sides.

2.1. Design

The numerical approach was carried out using Computational Fluid Dynamics with three-dimensional modeling. The dimensions in this modeling were carried out with dimensions of 1 m in length, 0.16 m in shell diameter, and 24 tubing diameters of 19 mm. The tubes are arranged in a square pattern with a distance of 24 mm on each tube. The inlet and outlet diameter for each fluid is 28 mm. The baffles used are three plate sections with a thickness of 5mm and a length of 65mm which are tilted at an angle of 45°. Each baffle has a distance of 10 mm and between each baffle arrangement there is a distance of 64 mm, so in total there are 13 baffle arrangements on the shell side. Each baffle arrangement is rotated 30° so that the shape resembles a helical.

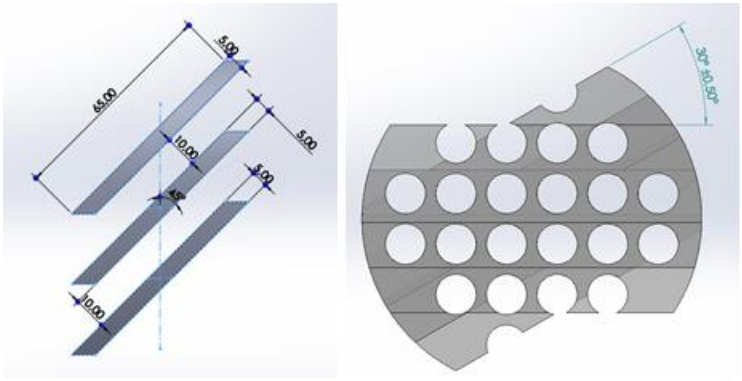

Figure 2. Baffle Arragement

2.2. Meshing

After making the model, it continues with the discretization (meshing) process using the tetrahedral type. Mesh quality is reviewed based on orthogonal quality with a range of 0.1-1. The mesh size influ-ences the achievement of convergence, so an independence test is carried out so that the simulation results do not deviate from the ideal value [13]. The results of the independence test are shown in Table 1. With an element size of 0.004, 1237899 element nodes were produced. The results of the inde-pendent test are used as a basis for determining element size in CFD simulations.

Tabel 1, Grid Independence Test

Element Size	heat transfer coefficient	error
0.010	1124.540	-
0.008	1126.2	0.15
0.006	1127.52	0.12
0.004	1128.08	0.05

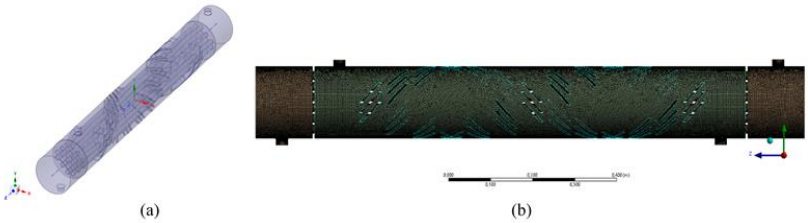

Figure 2. (a) STHeX Inclined Segmental Baffles model (b) Genereted mesh

2.3. CFD Simulation

Then, the results of the mesh stage are carried out by an initial definition process using the steady state and gravity parameters of the model. Defining the turbulence model using the Reynolds-Averaged Navier-Stokes (RANS) and the energy equation are also included in the computational process. The boundary conditions are set by entering the cold fluid inlet velocity (Vin s) in the range of 0.5-1.5 m/s and at the hot fluid inlet the velocity (Vin t) is constant at 0.2 m/s. Velocity and pressure modeling using the SIMPLE velocity-coupling method and a pressure-based solver are adopted Computational results were carried out using CFD-Post. Then the results of the numerical approach are validated against theoretical calculations (Figure. 3). In the figure it can be seen that the average deviation value is 12.024%.

2.4. Governing Equation

CFD is a calculation in fluid dynamics that is based on governing equations which represent mathematical equations from the conservation laws of physics. Understanding more of the fundamentals of fluid flow processes makes it easier to reach solutions in CFD easily. The boundary conditions of physics and the corresponding mathematical approaches will develop into precise forms of numerical calcu-lations.

The finite volume method is used in the conservation equations of mass, momentum, and energy. There are several turbulence models available in the program. The use of this method is increasingly widespread and is accepted by many parties as a method that is based on physics and is quite accurate and does not require a long time in numerical calculations. This method focuses on averaging operations, so that instantaneous fluctuations can be eliminated. The input average operation cuts time so that the results of numerical calculations can be known and match the existing equations. In two di-mensions the equations of continuity and conservation of momentum and energy resulting from the average values can be written [14]:

$$\frac{\partial \rho}{\partial t} + \frac{\partial (\rho \bar{u})}{\partial x} + \frac{\partial (\rho \bar{v})}{\partial y} = 0 \quad (1)$$

$$\frac{\partial (\rho \bar{u})}{\partial t} + \frac{\partial (\rho \bar{u}\bar{u})}{\partial x} + \frac{\partial (\rho \bar{v}\bar{u})}{\partial y} = \frac{\partial \bar{p}}{\partial x} + \frac{\partial}{\partial x}\left(\mu \frac{\partial \bar{u}}{\partial x}\right) + \frac{\partial}{\partial y}\left(\mu \frac{\partial \bar{u}}{\partial y}\right) + \frac{\partial}{\partial x}\left[\mu \frac{\partial \bar{u}}{\partial x}\right] + \frac{\partial}{\partial y}\left[\mu \frac{\partial \bar{v}}{\partial y}\right] - \left[\frac{\partial (\rho \overline{u'u'})}{\partial x} + \frac{\partial (\rho \overline{u'v'})}{\partial y}\right] \quad (2)$$

$$\frac{\partial (\rho \bar{v})}{\partial t} + \frac{\partial (\rho \bar{u}\bar{v})}{\partial x} + \frac{\partial (\rho \bar{v}\bar{v})}{\partial y} = \frac{\partial \bar{p}}{\partial x} + \frac{\partial}{\partial x}\left(\mu \frac{\partial \bar{v}}{\partial x}\right) + \frac{\partial}{\partial y}\left(\mu \frac{\partial \bar{v}}{\partial y}\right) + \frac{\partial}{\partial x}\left[\mu \frac{\partial \bar{u}}{\partial x}\right] + \frac{\partial}{\partial y}\left[\mu \frac{\partial \bar{v}}{\partial y}\right] - \left[\frac{\partial (\rho \overline{u'v'})}{\partial x} + \frac{\partial (\rho \overline{v'v'})}{\partial y}\right] \quad (3)$$

$$\frac{\partial (\rho \bar{T})}{\partial t} + \frac{\partial (\rho \bar{u}\bar{T})}{\partial x} + \frac{\partial (\rho \bar{v}\bar{T})}{\partial y} = \frac{\partial}{\partial x}\left(\frac{k}{C_p}\frac{\partial \bar{T}}{\partial x}\right) + \frac{\partial}{\partial y}\left(\frac{k}{C_p}\frac{\partial \bar{T}}{\partial x}\right) - \left[\frac{\partial (\rho \overline{u'T'})}{\partial x} + \frac{\partial (\rho \overline{v'T'})}{\partial y}\right] \quad (4)$$

Theoretical calculations on the STHeX segmented baffle use the Bell-Delaware method to calculate the heat transfer coefficient and pressure drop on the STHeX. The Bell Delaware method, which effect for fluid flow losses, was chosen for calculations as it is more reliable for practical scenarios. The Bell-Delaware method focuses on flow losses on the shell side [15]. Equation number (6) can be used to compute the heat transfer coefficient on the shell side. in formula (6), The value of J is the fluid flow leakage loss coefficient.

$$h_{id} = \frac{Nu_t \, x \, k_h}{d_i} \tag{5}$$

$$h_s = h_{id} J_c J_l J_b J_s J_r \tag{6}$$

3. RESULTS

Fluid flow velocity at the inlet shell produces mass flow rates of 0.301025 kg/s, 0.429801 kg/s, 0.600524 kg/s, 0.676239 kg/s, 0.859418 kg/s for STHeX Inclined Segmental Baffle respectively. Meanwhile, the mass flow rate on the tube side is constant at 0.1211 kg/s. Simulation results using AN-SYS show that the flow in STHeX forms a helical flow. As seen in Figure. 4, it can be seen that the fluid flow follows the shape of the baffle which has a slope angle at each baffle arrangement. The helical flow has a speed of about 0.81 m/s to 2.38 m/s, this value is much higher than the average flow that passes through the tube arrangement, but this is good for reducing the pressure drop on the shell side. The average speed of cold-water fluid washing the pipe is 0.025 m/s, 0.039 m/s, 0.058 m/s, 0.072 m/s, and 0.0891346 m/s respectively at different mass flow rates. The fluid flow speed is directly propor-tional to the heat transfer coefficient as seen in Figure. 3.

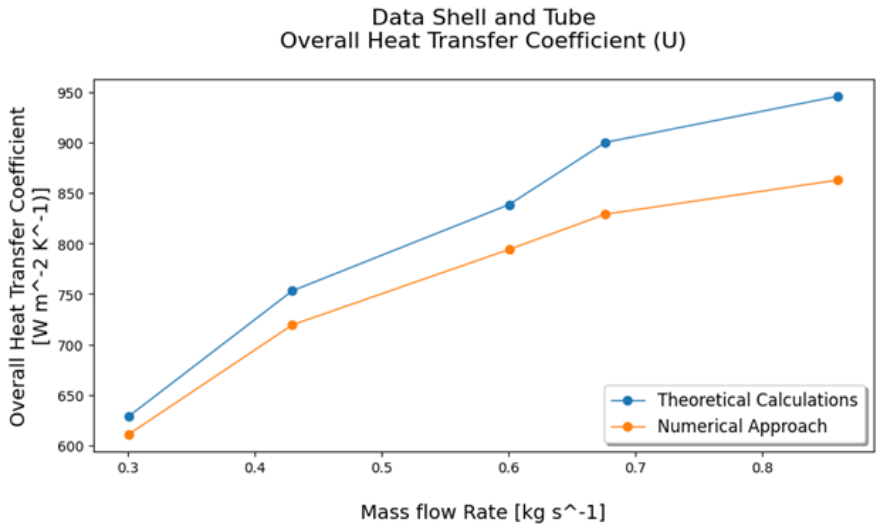

Figure 3. Comparison of simulation results and theoretical calculations for STHeX seg-mented baffle.

The heat transfer coefficient in Figure. 3 compares theoretical calculations with numerical simulations. The average deviation value between these two values is 5.8%. The highest deviation occurs at the highest mass flow rate, this is because there is a need to adjust the grid for each additional speed value. The simulation cost is directly proportional to the number of meshes, this is because a more detailed simulation will require more adequate hardware.

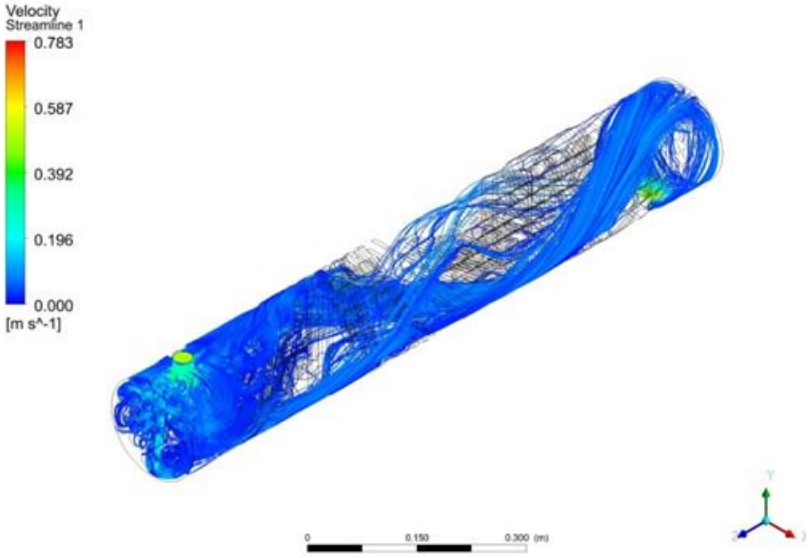

Figure 4. Streamline cold water fluid on shell side

4. DISCUSSION

Then, to see the flow characteristics, you need to look in more detail at the plan for each baffle. As seen in Figure. 5 that the longitudinal flow velocity in the z-axis direction is found in the top gap of the baffle to the shell surface and the gap below the baffle to the shell surface. Every change in angle in the baffle arrangement changes the direction of flow so that the flow in the gap is not uniform. This non-uniformity is caused by the empty gap between each baffle arrangement and the next baffle arrangement. On the middle side of the tube arrangement, the speed tends to be lower because the baffle arrangement blocks fluid flow in that section.

The velocity vector in Figure 5 (b) shows that the direction of fluid flow only washes one tube in area Y_1 and two tubes in area Z_1 so that the heat transfer in these two tubes has a fairly high thermal coefficient. This is because the higher the speed, the higher the Reynolds value and the resulting coefficient is greater than on other tubes. As can be seen in Figure 8 (b), the temperature of the cold air fluid increases in the section with the flow velocity in the middle section. The high velocity of fluid flow in the longitudinal flow direction makes the movement of heat tend to be smaller.

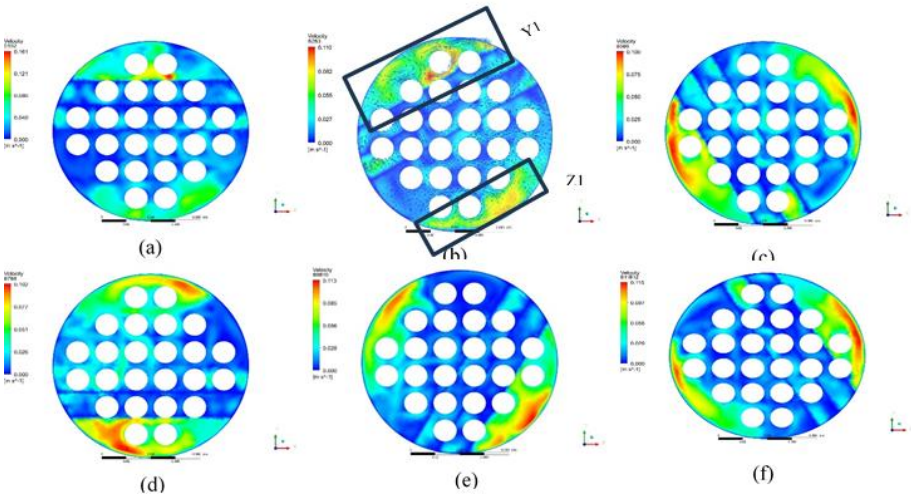

Figure 5. Velocity contours between baffles, (a) first and second baffles, (b) third and fourth baffles, (c) fifth and sixth baffles, (d) seventh and eighth baffles, (e) ninth and tenth baffles and (f) baffles eleventh and twelfth

Pressure drop on STHeX Inclined Segmental Baffles is depicted in Figure. 6. Where the highest pressure is in areas Y_2 and Z_2 where the baffle is tilted. Meanwhile, parts that have low pressure are a form of pressure drop caused by the presence of baffles. Each baffle has different pressure losses due to the increase in angle in each baffle arrangement.

Pressure drop is a factor that greatly influences the operation of a STHeX [16]. This is because the greater the pressure drop in STHeX, the additional energy required to flow the fluid to reach the desired pressure in the next process. Some STHeX applications in industrial installations involve several levels of SHTeX. Pressure drops at STHeX in multilevel installations will result in significant energy losses.

Another parameter to see the reliability of STHeX is to look at the overall summer growth coefficient. The overall heat transfer coefficient (U) is how much heat energy is transferred from one fluid to another fluid. The correlation between U and pressure drop (ΔP) can be seen in Figure 7 which com-pares U/ΔP on conventional STHeX segmented baffles with STHeX Inclined Segmental Baffles.

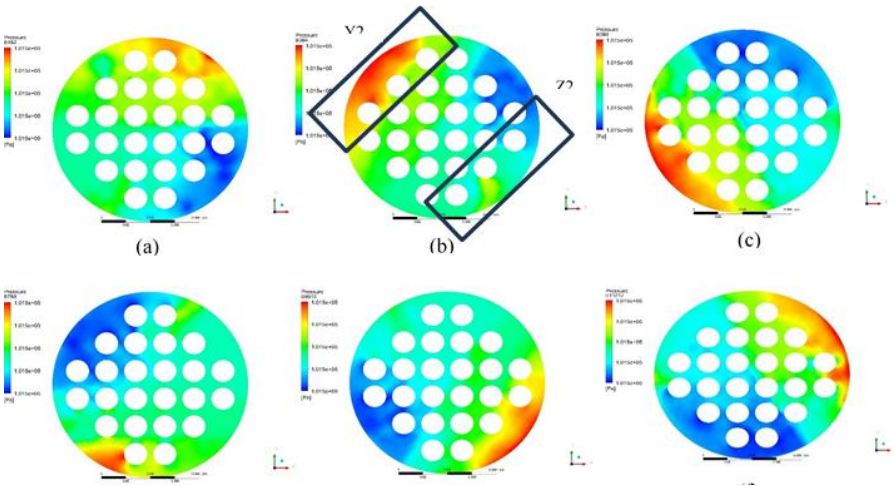

Figure 6. Pressure contours between baffles (a) first and second baffles, (b) third and fourth baffles, (c) fifth and sixth baffles, (d) seventh and eighth baffles, (e) ninth and tenth baffles and (f) eleventh and twelfth

In Figure. 7 it can be seen that as the mass flow rate increases, the U/ΔP value decreases for each STHeX that is compared. This is because the values of U and ΔP are directly proportional to the mass flow rate of a STHeX. With increasing mass flow rate the difference between the two is quite constant, around 34.77%. At a mass flow rate of 0.85, the biggest difference between the two STHeX is 37.18%. Thus the energy required on multilevel STHeX will be smaller on STHeX with Inclined Segmental Baffles compared to STHeX segmented baffles.

This phenomenon occurs because the fluid flow velocity in the STHeX segmented baffle which passes through the tube arrangement is higher than the fluid flow velocity in the STHeX with Inclined Segmental Baffles. As seen in Figure. 8 (c) at a speed of 0.858 is on a wider surface. Thus the heat transfer coefficient in that area is quite high which results in lower heat transfer in that area, which can be seen in Figure. 8(c). On the other hand, the fluid flow that does not pass through the baffle arrangement has the same speed so that there is no heat transfer in that area according to the figure in Figure. 8(c).

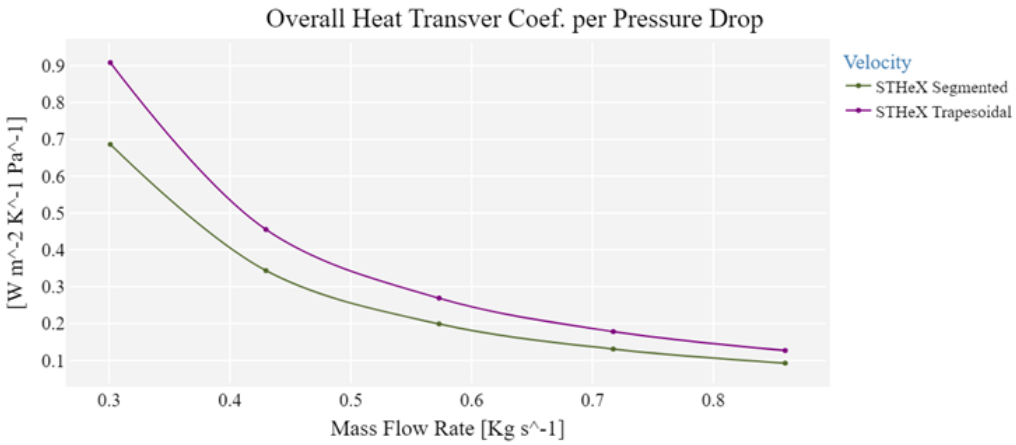

Figure 7. Overall coeficient heat transfer betwen konventional STHeX segmented baffle with STHeX Inclined Segmental Baffles

In Figure. 8 (a) The fluid flow flowing in the tube arrangement tends to be lower and the highest speed is only in the baffle gap area against the shell wall. Thus Figure. 8 (b) the heat transfer in the tube array is higher when compared to the STHeX segmented baffle Figure. 8 (c).

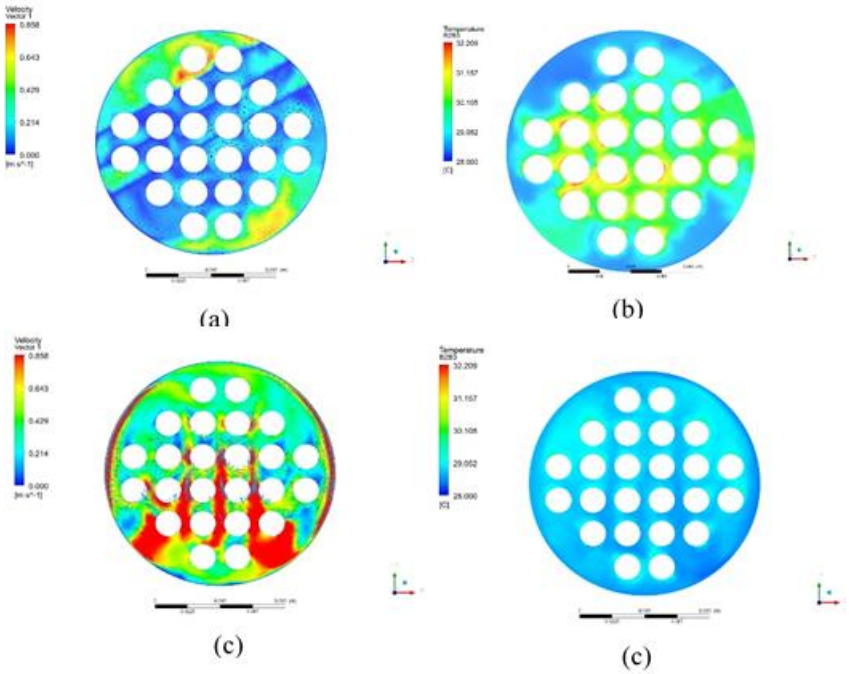

Figure 8. The difference between STHeX segmented baffle and STHeX Inclined Segmental Baffles in speed and temperature

After reviewing the temperature and heat transfer results, a review was carried out on the pressure drop between STHeX segmented baffles and STHeX Inclined Segmental Baffles. As seen in Figure. 9 that the pressure drop on the STHeX segmented baffle tends to be more constant with each additional baffle. This was also found in the different simulated mass flow rates. In contrast to STHeX Inclined Segmental Baffles, the phenomenon that forms with each additional baffle is quite fluctuating as the mass flow rate increases. This is because the flow does not pass through the gap between the baffles, but the fluid flows through the gap between the baffle and the shell wall.

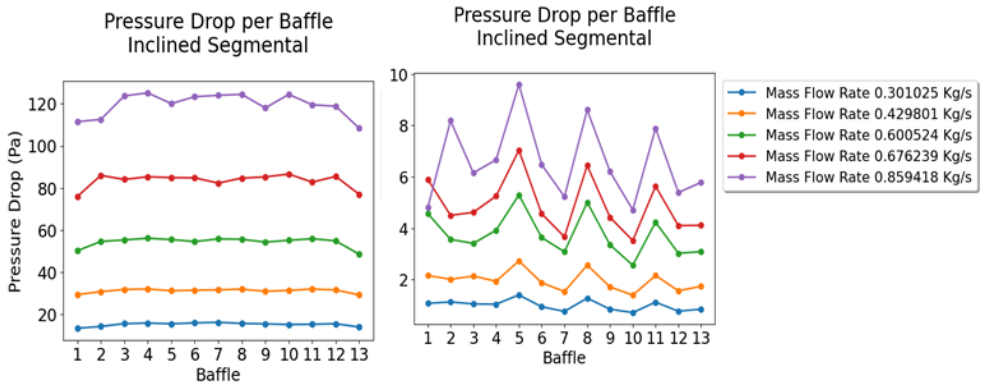

Figure 9. Pressure drop betwen konventional STHeX segmented baffle with STHeX Inclined Segmental Baffles

5. CONCLUSION

Shell and tube heat exchanger (STHeX) design development is ongoing in an effort to make the sys-tem more efficient. Investigating the best baffle design is one way to do this. Investigation of the new STHeX construction with inclined segment baffles was carried out.

Three-dimensional modeling and numerical approaches of CFD software were used to conduct the experiments. The pressure drop value is greatly reduced compared to standard STHeX, but the heat transfer coefficient value is lower. Deter-mination of the value of the total heat transfer coefficient per pressure loss (U/ΔP) is required. It is known that the average difference in U/ΔP values reaches 34.77% and the highest increase in value is 37.18% at a mass flow rate of 0.859 kg/s. Based on the results, STHeX with oblique segment partition improves.

REFERENCES

[1] R. V. Rao and A. Saroj, "Economic optimization of shell-and-tube heat exchanger using Jaya algorithm with maintenance consideration," Appl Therm Eng, vol. 116, pp. 473–487, 2017, doi: 10.1016/j.applthermaleng.2017.01.071.

[2] Z. H. Ayub, D. Yang, T. S. Khan, E. Al-Hajri, and A. H. Ayub, "Performance characteristics of a novel shell and tube heat exchanger with shell side interstitial twisted tapes for viscous fluids application," Appl Therm Eng, vol. 134, pp. 248–255, Apr. 2018, doi: 10.1016/j.applthermaleng.2018.01.054.

[3] X. Gu, W. Chen, Y. Fang, S. Song, C. Wang, and Y. Wang, "Analysis of flow dead zone in shell side of a heat exchanger with torsional flow in shell side," Appl Therm Eng, vol. 180, Nov. 2020, doi: 10.1016/j.applthermaleng.2020.115792.

[4] H. Kücük, M. Ünverdi, and M. Senan Yılmaz, "Experimental investigation of shell side heat transfer and pressure drop in a mini-channel shell and tube heat exchanger," Int J Heat Mass Transf, vol. 143, Nov. 2019, doi: 10.1016/j.ijheatmasstransfer.2019.118493.

[5] C. Yu, Z. Ren, and M. Zeng, "Numerical investigation of shell-side performance for shell and tube heat exchangers with two different clamping type anti-vibration baffles," Appl Therm Eng, vol. 133, pp. 125–136, Mar. 2018, doi: 10.1016/j.applthermaleng.2018.01.029.

[6] J. Ji, F. Li, B. Shi, and Q. Chen, "Analysis of the effect of baffles on vibration and heat transfer characteristics of elastic tube bundles," International Communications in Heat and Mass Transfer, vol. 136, Jul. 2022, doi: 10.1016/j.icheatmasstransfer.2022.106206.

[7] P. Stehlík, J. Němčanský, D. Kral, and L. W. Swanson, "Comparison of correction factors for shell-and-tube heat exchangers with segmental or helical baffles," Heat Transfer Engineering, vol. 15, no. 1, pp. 55–65, Jan. 1994, doi: 10.1080/01457639408939818.

[8] J. Wen, X. Gu, M. Wang, S. Wang, and J. Tu, "Numerical investigation on the multi-objective optimization of a shell-and-tube heat exchanger with helical baffles," International Communi-cations in Heat and Mass Transfer, vol. 89, pp. 91–97, Dec. 2017, doi: 10.1016/j.icheatmasstransfer.2017.09.014.

[9] H. Sasongko, H. Mirmanto, G. Bangga, E. F. Nugrahani, and J. N. Pasaribu, "numerical approach of the blade shape and number on the performance of multiple blade closed type impulse wind turbine," International Journal of Mechanical Engineering Technologies and Applications, vol. 4, no. 2, pp. 220–235, Jun. 2023, doi: 10.21776/mechta.2023.004.02.11.

[10] X. Gu, Y. Luo, X. Xiong, K. Wang, and Y. Wang, "Numerical and experimental investigation of the heat exchanger with trapezoidal baffle," Int J Heat Mass Transf, vol. 127, pp. 598–606, Dec. 2018, doi: 10.1016/j.ijheatmasstransfer.2018.07.045.

[11] J. Wen, H. Yang, S. Wang, S. Xu, Y. Xue, and H. Tuo, “Numerical investigation on baffle con-figuration improvement of the heat exchanger with helical baffles,” Energy Convers Manag, vol. 89, pp. 438–448, Jan. 2015, doi: 10.1016/j.enconman.2014.09.059.

[12] A. A. Abbasian Arani and R. Moradi, “Shell and tube heat exchanger optimization using new baffle and tube configuration,” Appl Therm Eng, vol. 157, Jul. 2019, doi: 10.1016/j.applthermaleng.2019.113736.

[13] D. E. Wahyudi, S. Nur’aini, W. K. Dewi, R. M. Aisyah, and E. L. Septiani, “The Calculation of Expense Reduction based on the Efficiency of Cyclone by Computational Fluid Dynamic,” In-ternational Journal of Mechanical Engineering Technologies and Applications, vol. 2, no. 2, p. 85, Jul. 2021, doi: 10.21776/mechta.2021.002.02.1.

[14] C. Ranganayakulu and K. N. Seetharamu, “Compact Heat Exchangers – Analysis, Design and Optimization using FEM and CFD Approach,” 2018.

[15] R. W. Serth, “Process Heat Transfer,” Kingsville, Texas, USA, 2007.

[16] Y. Lei, Y. Li, S. Jing, C. Song, Y. Lyu, and F. Wang, “Design and performance analysis of the novel shell-and-tube heat exchangers with louver baffles,” Appl Therm Eng, vol. 125, pp. 870–879, 2017, doi: 10.1016/j.applthermaleng.2017.07.081.